# Supporting Information

## Electrochemical $CO_2$ Reduction on Cu and Au Electrodes Studied through *in situ* Sum Frequency Generation Spectroscopy

*Zhi-Chao Huang-Fu, Qian-Tong Song, Yu-Han He, Jing-Jing Wang, Jin-Yu Ye, Zhi-You Zhou, Shi-Gang Sun* and Zhao-Hui Wang**

*Collaborative Innovation Center of Chemistry for Energy Materials, State Key Laboratory for Physical Chemistry of Solid Surface, Department of Chemistry, College of Chemistry and Chemical Engineering, Xiamen University, Xiamen 361005, China. E-mail: zhwang@xmu.edu.cn.*

### 1. SFG Setup and *in situ* Spectroelectrochemical Cell

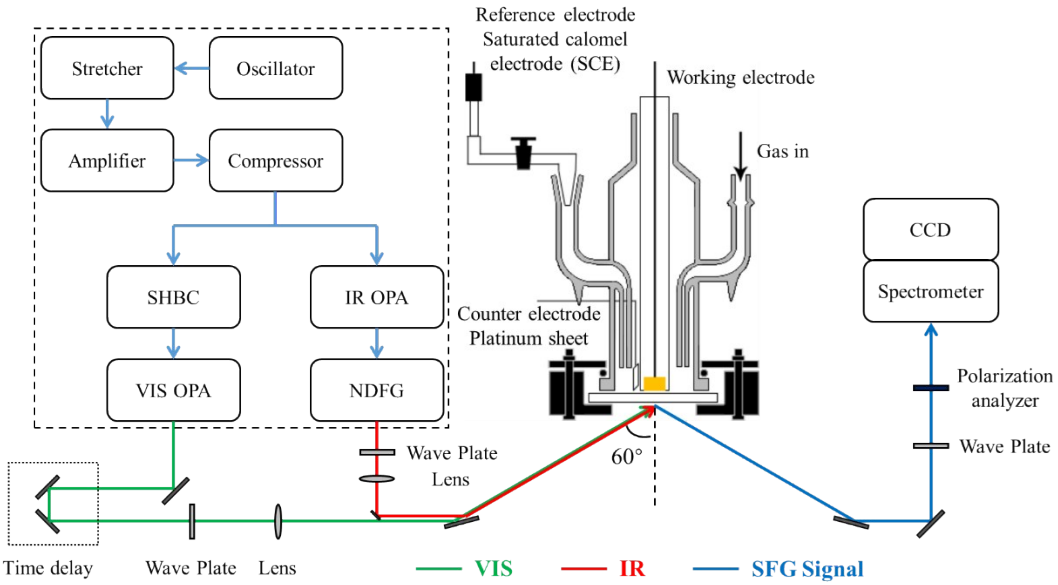


Figure S1 Schematic of the electrochemical BB-SFG setup.

The setup of our electrochemical BB-SFG was shown in Figure S1. A portion of the femtosecond Ti:Sapphire laser (Coherent Inc., Legend Elite Duo, 800 nm, ~100 fs, 1 KHz) was used to pump 2 optical parametric amplifiers (Light Conversion) to generate tunable broadband infrared pulses (IR, 2.6 ~ 10 μm, 150 fs, 160 $cm^{-1}$ FWHM) and narrow-band visible pulses (VIS, 470 ~ 900 nm, 2.5 ps, 7 $cm^{-1}$ FWHM). The IR and VIS were temporally and spatially overlap at

the sample surface with incident angles around 60 degrees. The SFG spectra were recorded by a spectrograph (Andor Technology, SR-303i-B) with a CCD detector (Andor Technology, DU920P-BR-DD).

We employed a home-built thin layer electrochemical cell constructed from a glass body sealed with a $CaF_2$ window (ϕ32 mm with 1 mm thickness) and fixed on a stainless steel base plate. The working electrodes were Cu and Au polycrystalline ϕ6 mm cylinders (Tianjin ida), which were embedded in PTFE holders with the metal surfaces exposing to the electrolytes. The electrode was pressed against the $CaF_2$ window to form a thin electrolyte layer (~ 20 μm in our measurements). A flame-annealed platinum sheet (99.99%) and a commercial saturated calomel electrode (SCE) electrode (Tianjin ida) served as the counter and reference electrodes, respectively. To investigate the surface species at different potentials, chronoamperometry performed to hold the electrode potential in the window of interest during the SFG measurements.

A 0.1 M $NaHCO_3$ solution (Sigma- Aldrich, in ultrapure $H_2O$, 18.2 MΩ·cm, Millipore Corporation) was used for *in situ* measurements of $CO_2$ reduction. During the $CO_2$ reduction process, $CO_2$ was bubbling into the cell to keep the saturation. CO adsorption measurement was conducted with 10 min pure CO (99.9%, Linde) bubbling into a 0.1 M $NaClO_4$ solution. Cyclic voltammetry (CV) measurements were carried out using a CHI604D potentiostat (CH Instruments).

**2. Electrochemical experiments.**

Before each electrochemical measurement, the Au and Cu electrodes were mechanically polished with alumina powder of sizes 5, 1, 0.3 μm successively, then cleaned in an ultrasonic bath. For the Cu electrode, one additional step of electropolishing in 85% phosphoric acid was adopted. The electrodes were then rinsed with ultrapure water for experimental measurements.

Figure S2 shows the cyclic voltammogram (CV) of the oxidation and reduction processes for a polycrystalline Au electrode at 50 $mV \cdot s^{-1}$ scanning speed in 0.5 M $H_2SO_4$ solution, which is in good agreement with that in the literature.[1, 2]

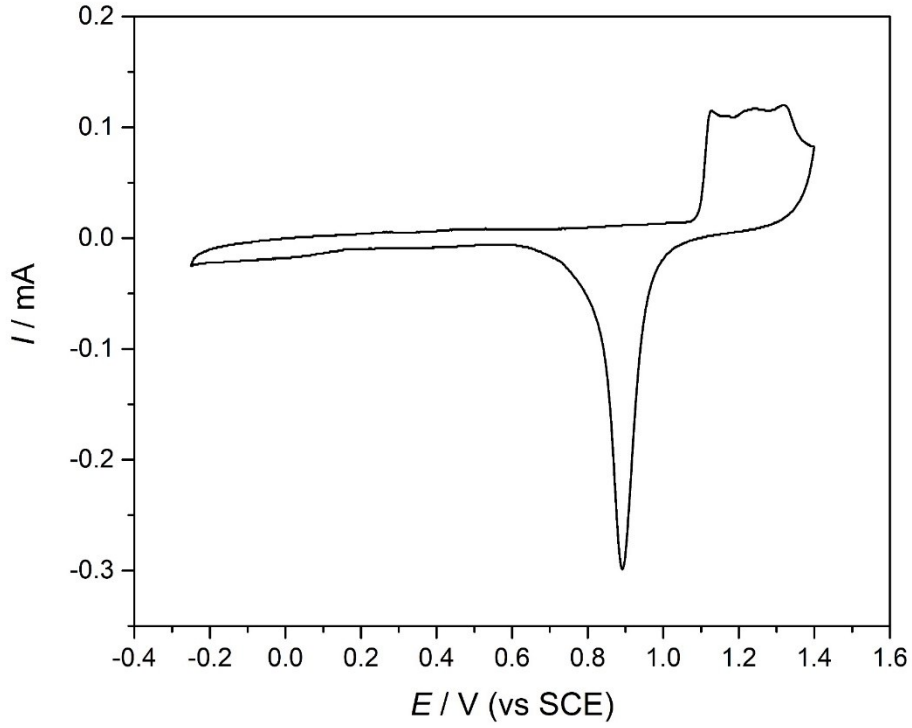


Figure S2 Cyclic voltammograms of the polycrystalline Au electrode in 0.5 M $H_2SO_4$ solution at 50 mV $s^{-1}$.

Figure S3 illustrates the CV of a polycrystalline Cu electrode recorded in 0.5 M $H_2SO_4$ solution. At potentials below -0.60 V, hydrogen evolution gives rise to the cathodic current. At potentials up on 0.00 V, a positive current appears and increases due to the Cu dissolution. These features match the previous results.[3]

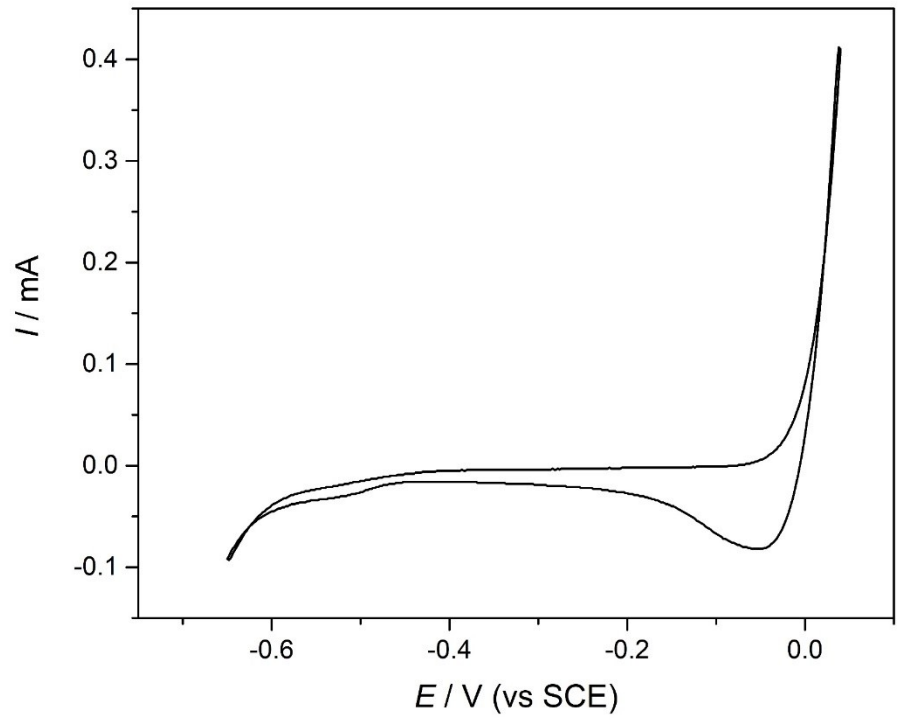


Figure S3 Cyclic voltammograms of the polycrystalline Cu electrode in 0.5 M $H_2SO_4$ solution at 50 mV $s^{-1}$.

Underpotential deposition (UPD) of Cu was performed on polycrystalline Au electrode. Figure S4 depicts the CV for Au electrode in 1 mM $CuSO_4$ + 0.5 M $H_2SO_4$ solution. The broad peak around 0.0 ~ 0.3 V is corresponding to Cu UPD. Then we held an Au electrode in 1 mM $CuSO_4$ + 0.5 M $H_2SO_4$ solution at 0.1 V for 60 s to complete the Cu UPD process. Figure S5 shows the Cu stripping on Cu-UPD/Au electrode, by calculating with the stripping charge quantity we can estimate the coverage area of Cu on Au from Eq. S1, and the results are listed in Table S1.

$$S_{Cu} = Q_{Cu} / (420\ \mu C \cdot cm^{-2}) \qquad \text{Eq. S1}$$

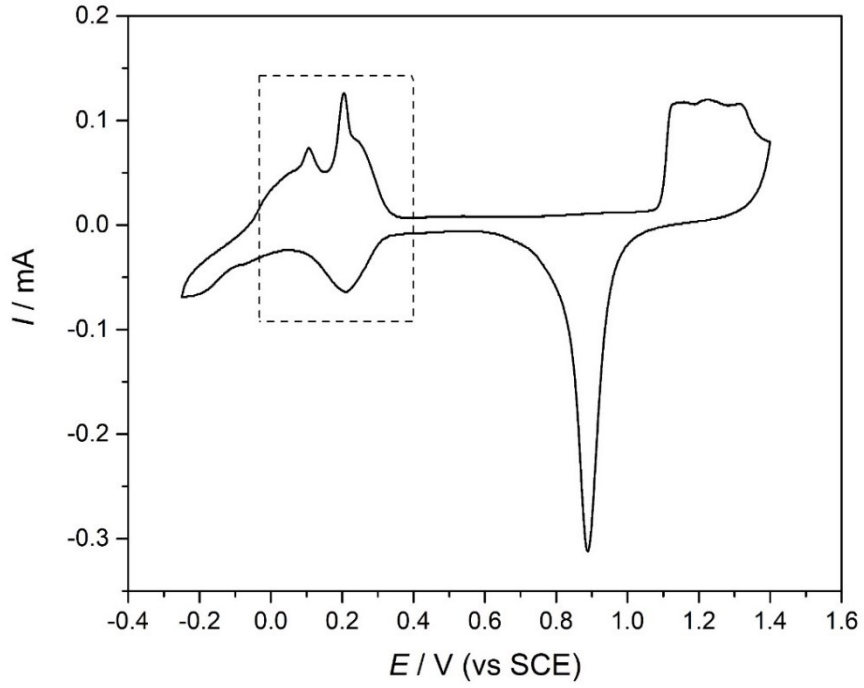


Figure S4 Cyclic voltammograms of the polycrystalline Au electrode in 1 mM $CuSO_4$ + 0.5 M $H_2SO_4$ at 50 mV $s^{-1}$.

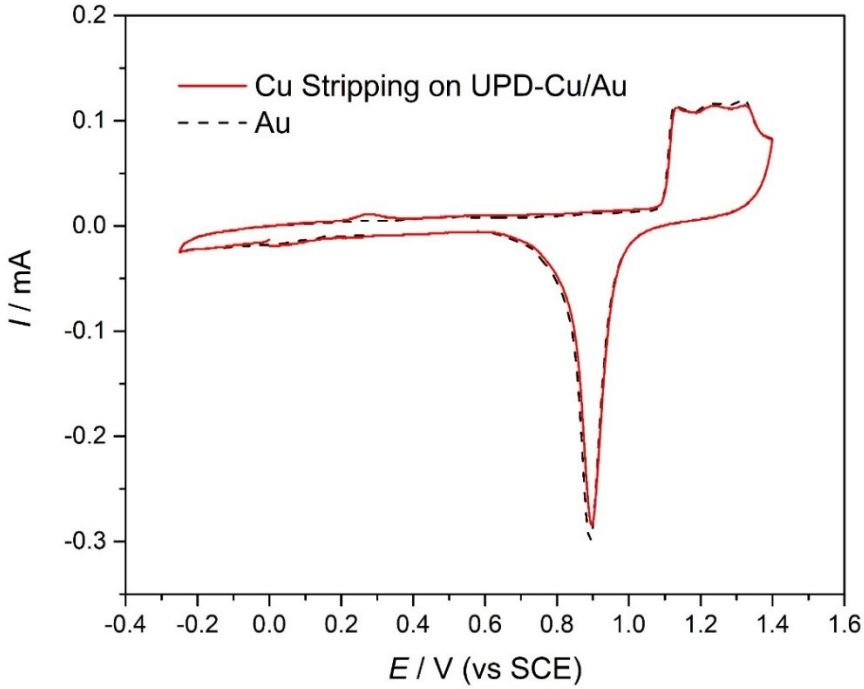


Figure S5 Cu stripping on UPD-Cu/Au in 0.5 M $H_2SO_4$ solution (Comparison with cyclic voltammograms of the Au electrode).

Table S1 Calculation of coverage area of Cu on UPD-Cu/Au.

| | Stripping Current Quantity (μC) | Coverage Area ($cm^{-2}$) |
|---|---|---|
| UPD-Cu/Au | 17.7 | 0.0421 |

**3. BB-SFG spectra fitting and normalization**

The intensity of the SFG signal, $I_{SFG}(\omega)$, can be expressed as:

$$I_{SFG} \propto \left|P_{SFG}(\omega)\right|^2 = \left|\chi^{(2)} E_{IR} E_{VIS}\right|^2 \quad \text{Eq. S2}$$

where $P_{SFG}$ is the induced polarization and $\chi^{(2)}$ is the second order susceptibility:

$$\chi^{(2)} = \chi^{(2)}_{NR} + \chi^{(2)}_{R} = A_{NR} e^{i\theta} + \sum_q \frac{A_q}{\omega_{IR} - \omega_q + i\Gamma_q} \quad \text{Eq. S3}$$

where $A_q$, $\omega_q$ and $\Gamma_q$ are the oscillation strength, frequency and half width of the $q^{th}$ mode vibrations of the resonances, $A_{NR}$ is the oscillation strength of the nonresonant, $\theta$ is the phase difference between the resonant and nonresonant.

Now we use SFG spectra of Cu electrode surface in the C-H stretching spectral range during $CO_2$ reduction as an example to describe the SFG spectra fitting process. Open circles in Figure S6 shows the raw SFG spectra. At -0.6 V, the BB-SFG spectrum is dominated by nonresonant contribution of the Cu electrode surface, a structure-less broadband feature, which represents the input IR spectral profile. After -0.8 V, new spectral features, two narrow SFG bands superimposed on the broad Cu SFG band. To better analyze the evolution of the resonant SFG bands, Eq. S4 has adopted to fit the BB-SFG spectra, the fitting results are solid lines in Figure S6.

$$I_{SFG} = \left| \left( A_{NR} + \sum_j \frac{A_R e^{i\theta_j}}{\omega_{IR} - \omega_j + i\Gamma_j} \right) exp\left( -\left( \frac{\omega_{IR} - \omega_0}{\sigma} \right)^2 \right) \right|^2 \quad \text{Eq. S4}$$

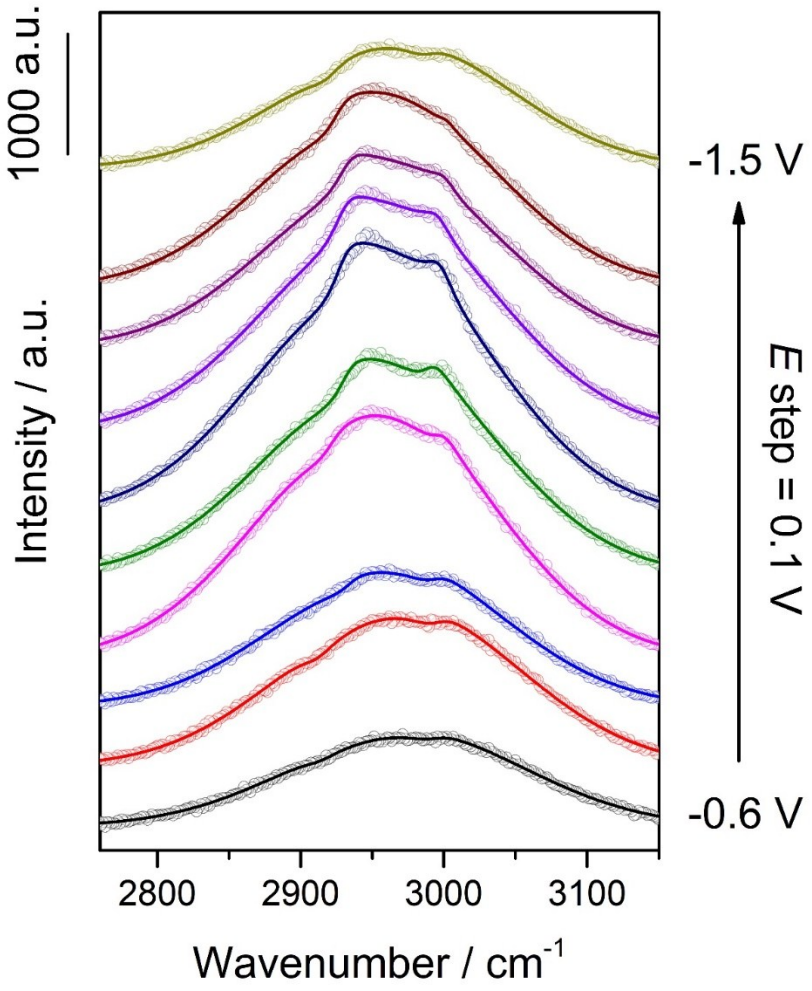


Figure S6 Potential-dependent BB-SFG spectra (C-H region) (open circles) and fitting data (solid lines) of $CO_2$ reduction in 0.1M $CO_2$-saturated $NaHCO_3$ solution at Cu electrode. Offset for comparison.

The final fitting parameters found for the spectra presented in Figure S6 are summarized in Table S2.

| $E$ (V) | $A_{NR}$ | $A_{R1}$ | $A_{R2}$ | $\theta_1$ (rad) | $\theta_2$ (rad) | $\omega_0$ ($cm^{-1}$) | $\omega_1$ ($cm^{-1}$) | $\omega_2$ ($cm^{-1}$) | $\sigma$ ($cm^{-1}$) | $\Gamma_1$ ($cm^{-1}$) | $\Gamma_2$ ($cm^{-1}$) |
|---|---|---|---|---|---|---|---|---|---|---|---|
| -0.6 | 27.5 | 5.0 | 1.7 | 2.6 | 5.7 | 2976.4 | 2963.7 | 3012.3 | 168.6 | 24.6 | 3.6 |
| -0.7 | 35.4 | 15.4 | 3.1 | 2.6 | 5.7 | 2972.7 | 2942.2 | 3016.6 | 169.1 | 30.0 | 5.7 |
| -0.8 | 33.3 | 18.1 | 38.1 | 0.9 | 1.4 | 2963.6 | 2943.7 | 2996.5 | 163.0 | 14.8 | 21.4 |
| -0.9 | 44.3 | 31.9 | 28.6 | 1.2 | 0.7 | 2954.3 | 2933.1 | 2999.2 | 165.5 | 19.1 | 14.1 |
| -1.0 | 40.6 | 54.4 | 32.5 | 1.0 | 0.3 | 2958.5 | 2936.9 | 2999.4 | 164.9 | 19.1 | 11.5 |
| -1.1 | 44.6 | 75.4 | 45.7 | 0.7 | 0.0 | 2954.4 | 2936.4 | 2998.5 | 165.0 | 19.7 | 13.7 |
| -1.2 | 42.0 | 51.6 | 20.6 | 0.6 | 5.7 | 2959.6 | 2934.6 | 2997.0 | 162.6 | 17.3 | 11.0 |
| -1.3 | 38.0 | 42.4 | 16.5 | 0.6 | 5.7 | 2960.6 | 2936.1 | 2998.5 | 162.0 | 15.6 | 11.5 |

| | | | | | | | | | | | |
|---|---|---|---|---|---|---|---|---|---|---|---|
| -1.4 | 39.0 | 48.9 | 1.5 | 1.1 | 5.7 | 2957.6 | 2934.6 | 3000.0 | 162.3 | 19.8 | 5.0 |
| -1.5 | 31.3 | 10.3 | 1.7 | 0.9 | 5.7 | 2971.9 | 2939.1 | 3009.8 | 161.2 | 8.4 | 2.0 |

Table S2. Fitting parameters for SFG spectra shown in Figure S6.

All the resonant bands in the main text are the reconstructed spectra from the parameters of resonant vibrations.

Nonresonant contribution of the Cu electrode surface is a structure-less broadband feature, which could represent the input IR spectral profile. We got the shape of nonresonant background from the spectrum that surface reaction or adsorption did not start. Then we obtain the normalized SFG spectra which could show resonant SFG features clearly.

**4. Supplementary BB-SFG spectra**

As noted in the main text, while CO bubbled to the Au electrode directly, SFG band of $CO_L$ was observed. However, when we tested the Cu electrode, in both C-H and CO region, no resonant bands could be observed as shown in Figure S7. Such results may indicate that CO cannot form an ordered adsorption structure on Cu.

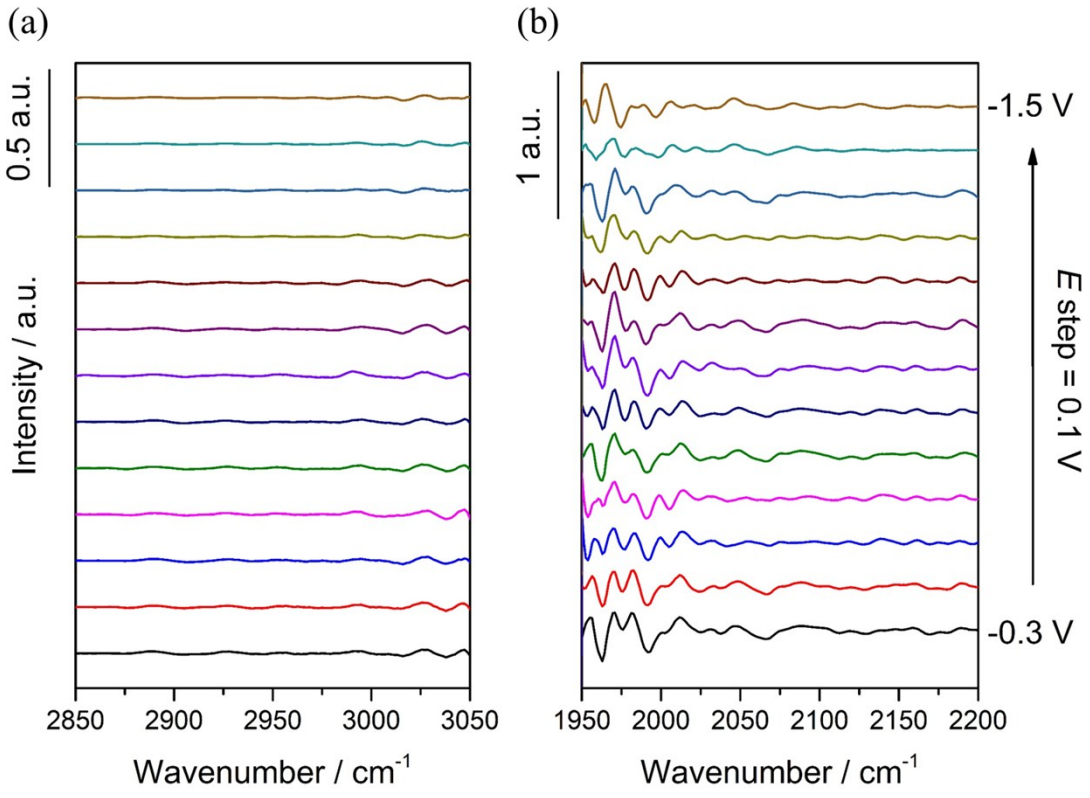

Figure S7 Potential-dependent normalized BB-SFG spectra in (a) C-H region and (b) CO region for CO adsorbed on polycrystalline Cu electrode in 0.1 M $NaClO_4$ solution. Offset for comparison.

Figure S8 displayed the spectra of Au electrode in 3 M ethanol solution (C-H region) and ultrapure water at open circuit potential (OCP). By contrast, two resonant features around 2930 and 2995 $cm^{-1}$ could be observed. These features are the resonant SFG bands from the interfacial ethanol molecules. The two SFG bands can also be assigned to $CH_2$-*as* and $CH_3$-*as* similar as the detected species during the $CO_2$ reduction in the main text, which blue-shifted due to the interfacial adsorption condition.[4] This comparison strongly suggests that the C-H features observed during the $CO_2$ reduction on Cu surface were from a structure similar to interfacial ethanol. Therefore, combined with the proposed mechanism on Cu,[5-7] we can conclude that the ethoxy intermediate leading to ethanol was directly observed on Cu.

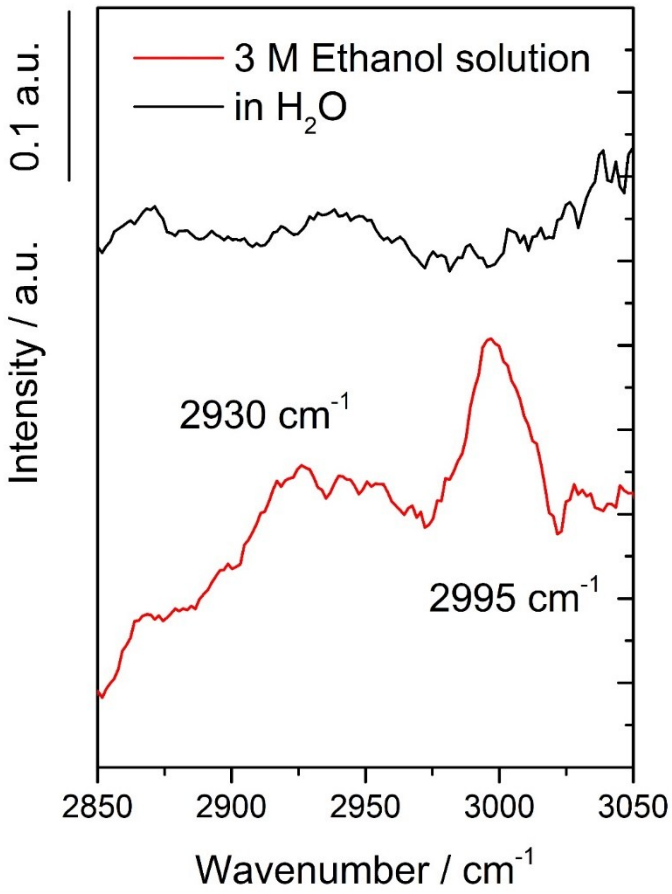


Figure S8 Normalized BB-SFG spectra (C-H stretching region) of an Au electrode in 3 M ethanol/water solution and ultrapure water at OCP.

**5. Electrochemical *in situ* FTIR spectroscopy**

Electrochemical *in situ* FTIR spectroscopy (*in situ* FTIRS) experiments in an attenuated total reflection (ATR) configuration were performed on a Nicolet 8700 Infrared spectrometer (Nicolet) equipped with a liquid nitrogen cooled MCT-A detector. Details of our *in situ* FTIRS studies have been reported elsewhere.[8, 9] The Cu film on Si was prepared by a seeded-growth procedure.[10] The spectra were collected using multistep FTIR spectroscopy (MSFTIRS) procedures. The results are presented in the form of relative change in reflectivity, i.e.

$$\frac{\Delta R}{R} = \frac{R(E_S) - R(E_R)}{R(E_R)} \qquad \text{Eq. S5}$$

where $R(E_S)$ and $R(E_R)$ are single-beam spectra of the reflection collected at sample potential $E_S$ and reference potential $E_R$, respectively. Spectral resolution in this study was 8 $cm^{-1}$ and each spectrum was coadded 200 interferograms (42 s). MSFTIRS spectra collected during the cathodic scan of the Cu film in a $CO_2$-saturated 0.1 M $NaHCO_3$ solution from -1.0 to -2.0 V are shown in Figure S9, reference spectrum was taken at -0.5 V. No absorption band was observed before -1.2 V. A band at ~2055 $cm^{-1}$ started to appear at -1.4 V, which was assigned to $CO_L$ on Cu film. Its intensity reached the maximum at −1.6 V and then gradually decreased. The band position of $CO_L$ initially blue-shifted and then red-shifted as the potential swept negatively, which was similar with the previous study by Zhu *et al*.[11] The broad feature and linewidth change were possibly related to the complicated environments of CO and the surface reconstructions of Cu during $CO_2$ reduction. In lower wavenumber region, a positive band corresponding to the consumption was observed. The band existed in the whole potential region and had no Stark tuning effect. Thus, it might come from the Cu-Si system. Bridged and multiply adsorbed CO were not detected. Our *in situ* FTIRS results indicate that CO was generated and linearly adsorbed on the Cu during $CO_2$ reduction.

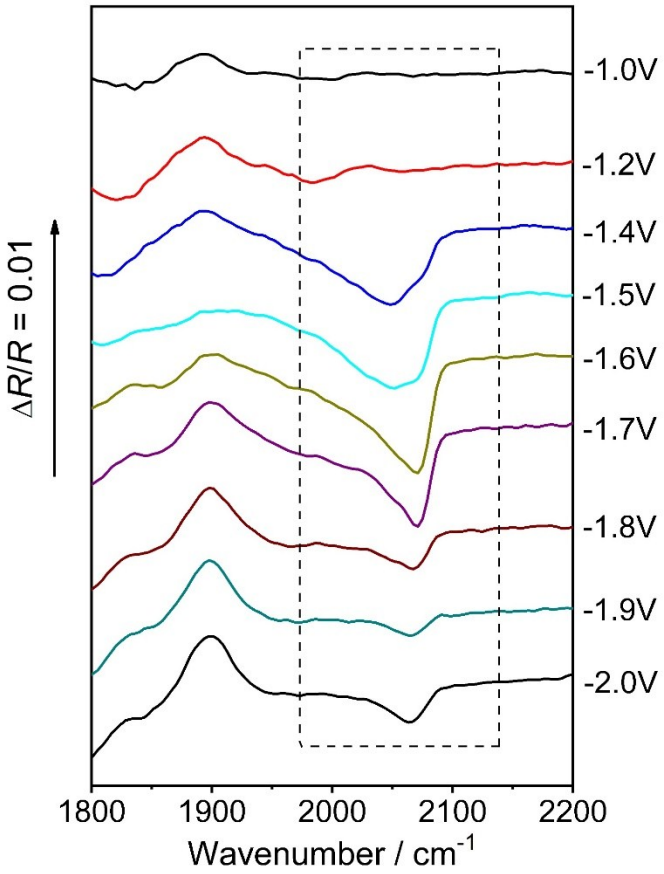


Figure S9 Potential-dependent MSFTIRS spectra of $CO_2$ reduction in 0.1M $CO_2$-saturated $NaHCO_3$ solution at Cu film electrode. Offset for comparison. Reference spectrum was taken at -0.5 V vs SCE.

**References:**


1. H. Angersteinkozlowska, B. E. Conway, A. Hamelin and L. Stoicoviciu, *Electrochimica Acta*, 1986, **31**, 1051-1061.
2. H. Angersteinkozlowska, B. E. Conway, A. Hamelin and L. Stoicoviciu, *Journal of Electroanalytical Chemistry*, 1987, **228**, 429-453.
3. M. R. Vogt, A. Lachenwitzer, O. M. Magnussen and R. J. Behm, *Surface Science*, 1998, **399**, 49-69.
4. R. Lu, W. Gan, B. H. Wu, Z. Zhang, Y. Guo and H. F. Wang, *J Phys Chem B*, 2005, **109**, 14118-14129.
5. R. Kortlever, J. Shen, K. J. Schouten, F. Calle-Vallejo and M. T. Koper, *J Phys Chem Lett*, 2015, **6**, 4073-4082.
6. F. Calle-Vallejo and M. T. Koper, *Angew Chem Int Ed Engl*, 2013, **52**, 7282-7285.
7. K. J. P. Schouten, Y. Kwon, C. J. M. van der Ham, Z. Qin and M. T. M. Koper, *Chemical*

*Science*, 2011, **2**, 1902-1909.

8. S.-G. Sun and Y. Lin, *Electrochimica Acta*, 1998, **44**, 1153-1162.
9. J.-Y. Ye, Y.-X. Jiang, T. Sheng and S.-G. Sun, *Nano Energy*, 2016, **29**, 414-427.
10. H.-F. Wang, Y.-G. Yan, S.-J. Huo, W.-B. Cai, Q.-J. Xu and M. Osawa, *Electrochimica Acta*, 2007, **52**, 5950-5957.
11. S. Zhu, B. Jiang, W.-B. Cai and M. Shao, *Journal of the American Chemical Society*, 2017, **139**, 15664-15667.